JACS
JOURNAL OF THE AMERICAN CHEMICAL SOCIETY

ARTICLE

pubs.acs.org/JACS

Formation Pathway of $CuInSe_2$ Nanocrystals for Solar Cells

Mahaprasad Kar,[†] Rakesh Agrawal,*[,†] and Hugh W. Hillhouse*[,†,‡]

[†]Chemical Engineering and the Energy Center, Purdue University, West Lafayette, Indiana 47907, United States

[‡]Chemical Engineering, University of Washington, Seattle, Washington 91805, United States

ABSTRACT: Copper, indium, and gallium chalcogenide nanocrystals (binary, ternary, and quaternary) have been used to fabricate high-efficiency thin-film solar cells. These solution-based methods are being scaled-up and may serve as the basis for the next generation of low-cost solar cells. However, the formation pathway to reach stoichiometric ternary $CuInSe_2$ or any chalcopyrite phase ternary or quaternary nanocrystal in the system has not been investigated but may be of significant importance to improving nanocrystal growth and discovering new methods of synthesis. Here, we present the results of X-ray diffraction, electron microscopy, compositional analysis, IR absorption, and mass spectrometry that reveal insights into the formation pathway of $CuInSe_2$ nanocrystals. Starting with CuCl, $InCl_3$, and elemental Se all dissolved in oleylamine, the overall reaction that yields $CuInSe_2$ involves the chlorination of the hydrocarbon groups of the solvent. Further, we show that the amine and alkene functional groups in oleylamine are not necessary for the formation of $CuInSe_2$ nanocrystals by conducting successful syntheses in 1-octadecene and octadecane. Hence, the role of oleylamine is not limited to nanocrystal size and morphology control; it also acts as a reactant in the formation pathway. Typically, the formation of copper selenide (CuSe) and indium selenide (InSe) nanocrystals precedes the formation of $CuInSe_2$ nanocrystals in oleylamine. But it was also found that $Cu_{2-x}Se$ ($0 < x < 0.5$) and In_2Se_3 were the primary intermediates involved in the formation of CISe in a purely non-coordinating solvent such as 1-octadecene, which points to the surface-stabilization effect of the coordinating solvent on the less thermodynamically stable indium selenide (InSe) nanocrystals. We also show that the yield of the chalcopyrite phase of $CuInSe_2$ (as opposed to the sphalerite phase) can be increased by reacting CuSe nanocrystals with $InCl_3$.

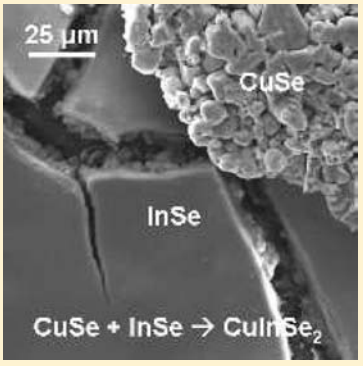

1. INTRODUCTION

$CuInSe_2$ (CISe) and related $Cu(In_{1-x}Ga_x)(S_{1-y}Se_y)_2$ materials ($0 \le x, y \le 1$) continue to receive considerable attention for applications in thin-film solar cells due to their unique structural and electrical properties[1,2] and their demonstrated high photovoltaic performance.[3] However, the high costs and the scale-up difficulties associated with vacuum-based fabrication processes have led researchers to investigate solution-phase processes based on the $Cu(In,Ga)(S,Se)_2$ family of nanocrystal inks to make low-cost solar cells.[4−11] The creation of suitable colloidal nanocrystal inks for use in a scalable coating process is a key step in the development of low-cost solar cells.[12,13] Notably, considerable progress has been made in semiconductor nanocrystal synthesis in recent years,[14−18] and there have been several reports describing the synthesis of CISe and related ternary and quaternary nanoparticles.[19−31] Recently, Guo et al. reported a solution synthesis of stoichiometric, chalcopyrite $CuInSe_2$ nanocrystals and a power conversion efficiency of 2.8% from solar cells made by consolidating the CISe nanocrystals into larger crystalline domains by a brief thermal treatment.[4] Insights into the formation pathway of the CISe nanocrystals would allow better control over the size and morphology of the nanocrystals and also might lead to discovery of new routes to synthesize the photoactive semiconductor.

Several methods have been reported in the literature for the synthesis of CISe and related nanoparticles, but very few attempts have been made investigate the formation pathway.[22,27,29,31,32] Xie and Qian's group[22] synthesized $CuInSe_2$ nanoparticles via a solvothermal route with ethylenediamine and speculated the reaction mechanism to involve $(InSe_2)^-$ and $Cu(en)_2^+$ (ethylenediamine complex of copper) as the intermediates. Gedanken and co-workers proposed a mechanism for the formation of microwave-assisted CISe nanoparticles involving the reaction of Cu (reduced from CuCl by polyol) with elemental In and Se releasing Cl_2 gas.[27] Chun et al.[29] reported the solvothermal synthesis of chalcopyrite-structured CISe and CIGSe nanoparticles and proposed a mechanism wherein selenium and copper first dissolved in ethylenediamine solvent to form Se^{2-} and $[Cu(en)_2]^+$ complexes, respectively. In and Ga (in their molten state) then reacted with the selenium to form In_2Se_3 and Ga_2Se_3 respectively, followed by their reaction with the Se^{2-} and $[Cu(en)_2]^+$ complexes to form CIGSe nanoparticles. Zhong's group synthesized selenium-deficient, chalcopyrite $CuInSe_2$ nanocrystals using alkanethiol as the ligand and octadecene as the non-coordinating solvent from CuCl, $InCl_3$, and TOPSe precursors.[31] They observed that both the metal-coordinating ligand and the non-coordinating solvent were necessary for the synthesis of CISe nanocrystals. More recently, Sargent's group[32] reported the synthesis of narrowly size-distributed CISe nanoparticles in

Received: May 8, 2011
Published: September 01, 2011

oleylamine using acetylacetonate precursors of Cu and In and elemental Se. They speculated the oxidation of oleylamine and the reduction of Cu^{2+} to Cu^{+} and Se to Se^{2-} to be the reaction mechanism. The reports mentioned above do provide some hypotheses for formation pathways and a sense for the breadth of possible syntheses, but there is little spectroscopic or analytical data to support the proposed formation pathways (evidence of specific solid intermediates or the metal−ligand intermediates). Further, these alternative synthesis routes have not yet yielded high-efficiency photovoltaic devices. From here forward, we restrict our discussion to the oleylamine route that has yielded good-performing photovoltaic devices.

Previously Guo et al.,[4,33] and more recently Panthani et al.,[7] reported the synthesis of stoichiometric, chalcopyrite $CuInSe_2$ nanocrystals using CuCl, $InCl_3$, and elemental Se using oleylamine as the sole solvent. The former also reported the formation of the sphalerite $CuInSe_2$ nanocrystals by simply altering the order of addition of one of the precursors. A film of the sphalerite CISe nanocrystals was then subsequently converted to the chalcopyrite crystal structure via a brief thermal treatment in selenium vapor.[4] The ordered chalcopyrite phase of $CuInSe_2$ is of most interest for photovoltaic applications. As such, it is important to understand the formation pathway to develop new routes to synthesize nanocrystals and thin-films of CISe.

If one assumes that the solvent is not involved in any of the chemical reactions, then (starting with chloride precursors and elemental Se) the overall reaction is

$$CuCl(s) + InCl_3(s) + 2Se(l) \rightarrow CuInSe_2(s) + 2Cl_2(g) \quad (1)$$

However, the Gibbs free energy of this reaction at 275 °C as calculated using HSC Chemistry software[34] is +309 kJ/mol. The fact that the free energy of this reaction is very thermodynamically unfavorable shows that this cannot be the correct formation pathway and that either the solvent is a likely active participant in the chemical reaction or solvation effects or surface interactions are dominant factors in the thermodynamics. Here, we present results from X-ray diffraction, electron microscopy, compositional analysis, FTIR, and mass spectrometry to investigate this question. We show that the solvent is an active participant in the reaction, in addition to any solvation effects or surface stabilization of nanocrystals. We also identify some of the intermediates observed during the synthesis and a method to synthesize chalcopyrite CISe nanocrystals in solvents without any metal-coordinating groups.

2. MATERIALS AND METHODS

2.1. Materials. Copper(I) chloride (99.995%), indium(III) chloride (99.999%), selenium (99.99%), oleylamine (technical grade, Fluka), octadecane (technical grade), 1-octadecene (technical grade), toluene (anhydrous), and ethanol (ACS reagent grade, >99.5%) were purchased from Aldrich (unless otherwise specified) and used without purification.

2.2. Synthesis. All manipulations were performed using standard air-free techniques. Chalcopyrite CISe nanocrystals were synthesized using a procedure similar to that reported by Guo et al.[4] In a typical synthesis, 7.5 mL of oleylamine was added to a 25 mL three-neck round-bottom flask connected to a Schlenk line apparatus, degassed around 130 °C and purged with Ar gas alternatively for three cycles. Next, 3 mL of 0.25 M solution of CuCl in oleylamine (CuCl−OLA), and 3 mL of 0.25 M solution of $InCl_3$ in oleylamine ($InCl_3$−OLA), and 1.5 mL of 1 M Se suspension in oleylamine were added to the reaction flask in the same order. The contents of the flask were then purged with argon and degassed alternatively for three cycles. Next, the temperature of the reaction mixture was raised to 275 °C, which typically took about 1 h. During this process, 1 mL aliquots of the reaction mixture were extracted from the reactor and quenched in a vial containing toluene for further analysis. These extracts were taken at temperatures of 130, 155, 180, 195, 210, 225, 250, and 275 °C. The temperature was then held for 30 min at 275 °C to allow for the growth of the CISe nanocrystals. After the reaction, the mixture was allowed to cool to 60 °C, after which toluene and ethanol were added to it and centrifuged at 10 000 rpm for 10 min. The supernatant was decanted and the nanocrystals were redispersed in toluene to form an ink.

CuSe crystals (hexagonal phase) and InSe nanocrystals (cubic phase) were synthesized using the same apparatus described above. For the synthesis of CuSe crystals, 7.5 mL of oleylamine was taken in the reaction flask at room temperature, and heated up to 130 °C, after which 2 mL of 0.25 M CuCl−OLA and 0.5 mL of 1 M Se−OLA were added to the reaction mixture. The contents were heated to 230 °C, which typically took about 45 min, and then immediately cooled back down to room temperature within a minute to suppress the formation of the $Cu_{2-x}Se$ phase. The $Cu_{2-x}Se$ phase is typically formed in higher quantities at extended reaction times. For the InSe nanocrystals, 7.5 mL of oleylamine was taken in the reaction flask at room temperature and heated to 130 °C, after which 2 mL of 0.25 M $InCl_3$−OLA and 0.5 mL of 1 M Se−OLA were added to the reaction mixture. The contents were heated to 275 °C, which typically took about 1 h. The nanocrystals were allowed to grow for 30 min at 275 °C, before cooling the reactor back to room temperature. Increasing the reaction time of the InSe nanocrystals beyond about 60 min led to the formation of In_2Se_3 phase.

In the synthesis of CISe nanocrystals using 1-octadecene and octadecane, a similar procedure was followed as mentioned for the synthesis in oleylamine. The only difference was that CuCl and $InCl_3$ powders (in the same quantity as before) were added to 13.5 mL of the solvent at room temperature, followed by three cycles of purging and degassing. The addition of 1.5 mL of 1 M Se suspension in 1-octadecene or octadecane was done at 130 °C.

2.3. Characterization. For characterization purposes, the nanocrystals were deposited on to appropriate substrates followed by the evaporation of toluene from the ink. The size and morphology of the nanocrystals were characterized using a FEI Nova NanoSEM field emission scanning electron microscope (FESEM). The phase and the crystallographic structure of the nanocrystals were characterized by powder X-ray diffraction (PXRD) using a Scintag X2 diffractometer (using Cu Kα radiation, λ = 0.15406 nm). The composition of the nanocrystals was analyzed by energy dispersive X-ray spectrometry (EDX) using an Oxford Inca250 EDS system built on a FEI Nova NanoSEM.

Matrix-assisted laser desorption ionization (MALDI) mass spectrometry was used to identify fragile byproduct of the reaction using an Applied Biosystems Voyager DE Pro mass spectrometer. This instrument utilizes a nitrogen laser (337 nm UV laser) for ionization with a time-of-flight mass analyzer. The positive ion mass spectra were obtained in the linear mode. The accelerating voltage was set at 20 kV and the grid voltage at 85%. The matrix used for these samples was α-cyano-4-hydroxycinnamic acid. The sample and matrix were mixed in a ratio of 1 μL:1 μL on the sample plate. This mixture was allowed to air-dry prior to insertion into the mass spectrometer for analysis. Fourier transform infrared (FTIR) spectra of the reaction mixture and the surfacatant-capped nanocrystals were obtained using a Nexus 670 spectrometer. For MALDI mass spectrometry and FTIR spectroscopy analysis, the liquid phase of the reaction mixture was collected after the separation from the solid-phase using centrifugation. For these measurements specifically, the concentration of all the precursors in oleylamine

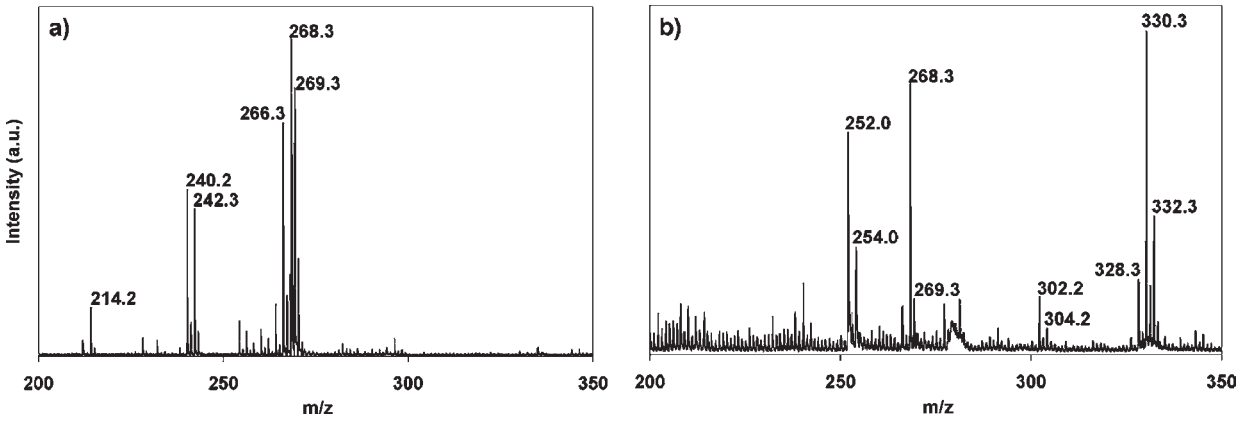

Figure 1. MALDI mass spectrometry of (a) oleylamine and (b) reaction supernatant collected at the start (130 °C) of the reaction.

during the synthesis was roughly doubled to get a better signal-to-noise ratio of the byproduct in the reaction mixture. For FTIR analysis of the liquid phase in the transmission mode, a few microliters of the supernatant were placed on a AgCl window. For the nanocrystals, samples were prepared by drop-casting a dispersion of the nanocrystals (in toluene) on a AgCl window and letting the solvent evaporate. GC-MS spectra of the liquid phase were collected with a Agilent 5975C mass spectrometer system. Typical electron energy was 70 eV with the ion source temperature maintained at 250 °C. The individual components were separated using a 30 m HP-5 capillary column (250 μm i.d. × 0.25 μm film thickness). The initial column temperature was set at 150 °C (for 0.1 min) and programmed to 300 at 10 °C/min. The flow rate was typically set at 1 mL/min. The injector temperature was set at 250 °C. Methane was used as the reagent gas for the chemical ionization analyses. The quantitative analysis of the byproduct formed in the liquid phase of the reaction mixture was done by comparing the GC spectrum of a sample with a known concentration of the chlorinated compound with the spectrum of the reaction supernatant with an unknown concentration. Standards with 0.02 and 0.05 molar ratios of 1-chlorooctadecane in octadecane and 1-octadecene were used.

3. RESULTS AND DISCUSSION

3.1. Reaction in Coordinating Oleylamine Solvent. The starting solvent and the supernatant from the reaction mixture were analyzed using Matrix-assisted laser desorption ionization (MALDI) mass spectrometry and FTIR spectroscopy to investigate the chemical changes during the reaction. MALDI was used to detect the formation of fragile byproducts of the reaction in the liquid phase. Figure 1a shows the mass spectrum of as-received oleylamine (OLA = $C_{18}H_{37}N$), with m/z peaks at 268.3 corresponding to the molecular weight of the $[C_{18}H_{37}N-H]^+$ ion. The rest of the peaks in the spectrum are typical of technical-grade purity oleylamine and are mainly due to the presence of other amines with varying carbon chain lengths. Quantification of the MALDI spectrum of the as-received oleylamine gave the following constituents and compositions: oleylamine, 71%; $C_{16}H_{31}NH_2$, 7.5%; hexadecylamine, 6.5%; octadecylamine, 6%; C_{14}-amine, 2%; C_{12}-amine, 2%; C_{17}-amine, 1.5%; C_{11}-amine, 1%; and C_9-amine, 1%.

The mass spectrum of the reaction supernatant is shown in Figure 1b, which consists of the $[C_{18}H_{37}N-Cu]^+$ ion with a m/z ratio of 330 and an isotope at 332, whose intensity ratio matches with that of the copper isotopes (2.2:1). The other ion that was identified in the mass spectrum of the supernatant belongs to the chlorinated oleylamine molecule $[Cl-C_{18}H_{36}N-H]^+$ which has a corresponding m/z ratio of 302 and an isotope at 304, and whose intensity ratio matches closely with that of the chlorine isotopes (3:1). No complexes of indium or selenium with oleylamine were detected. Table 1 lists all the ionized molecules observed in significant quantities in both the spectra.

Table 1. Observed m/z Peaks in the MALDI Spectra of Pure Oleylamine (Figure 1a) and the Reaction Supernatant (Figure 1b) and Their Corresponding Ionized Molecules

m/z	ion
330.3, 332.2	$[C_{18}H_{37}N-Cu]^+$
302.2, 304.2	$[Cl-C_{18}H_{36}N-H]^+$
268.3	$[C_{18}H_{37}N-H]^+$
266.3	$[C_{18}H_{35}N-H]^+$
254.0	$[C_{18}H_{37}-H]^+$
252.0	$[C_{18}H_{35}-H]^+$
242.3	$[C_{16}H_{35}N-H]^+$
240.2	$[C_{16}H_{33}N-H]^+$
214.2	$[C_{14}H_{31}N-H]^+$

FTIR spectroscopy was used to identify the functional groups present in the byproducts that were formed in the liquid phase during the reaction. Figure 2 compares the transmission FTIR spectrum of oleylamine (Figure 2a) with that of the reaction supernatant (Figure 2b) and a film of the as-synthesized CISe nanocrystals (Figure 2c).

Table 2 lists the wavenumbers corresponding to the vibrational modes (ν indicates stretching modes and δ deformation modes, where subscripts "s" and "a" stand for symmetric and asymmetric vibration modes correspondingly) of the functional groups identified in Figure 2.

The FTIR spectrum of the reaction supernatant (Figure 2b) shows the presence of broadened peaks in the wavenumber range of 3100−2600 cm^{-1} as well as the appearance of a wide band around 2164 cm^{-1}, both of which are characteristics of a protonated amine group (N^+-H vibration modes).[35] This spectrum matches well with that of an alkylamine hydrochloride[35] (in this case oleylamine), which suggests that hydrogen chloride is one of the byproducts that reacts with the excess oleylamine to form the oleylamine hydrochloride salt.

In the CISe nanocrystals' spectrum (Figure 2c), stretching modes corresponding to the C−Cl bond were observed at

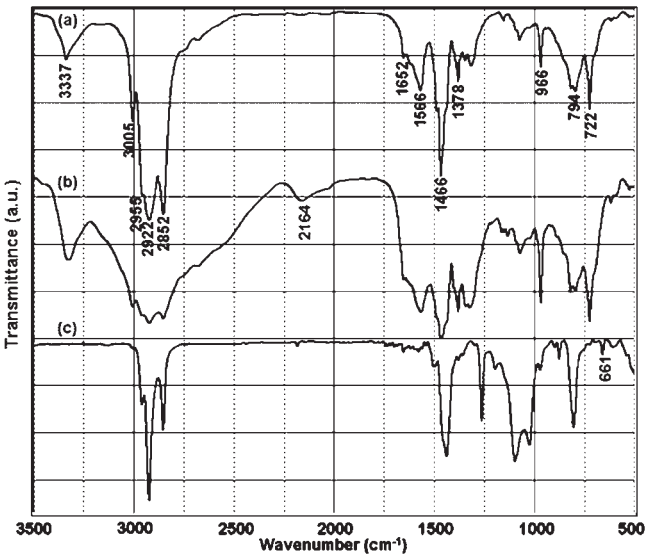

Figure 2. FTIR transmission spectra of (a) oleylamine, (b) reaction supernatant, and (c) the oleylamine-capped CISe nanocrystals showing the vibration modes in the latter (661 cm^{-1}) owing to the presence of the C−Cl bond.

Table 2. Vibrational Modes Observed in the FTIR Spectra of Oleylamine Shown in Figure 2a

wavenumber (cm^{-1})	vibrational modes	reference
3337	ν_s (NH_2)	3335 cm^{-1} [35]
3005	*cis* ν_s (−CH═)	3006 cm^{-1} [36]
2955	ν_a (CH_3)	2954 cm^{-1} [37]
2922	ν_a (CH_2)	2922 cm^{-1} [36]
2852	ν_s (CH_2)	2854 cm^{-1} [36]
2164	unidentified	2220−1820 cm^{-1} [35]
1652	ν (C═C)	1647 cm^{-1} [36]
1566	δ_s (NH_2)	1593 cm^{-1} [36]
1466	δ_s (CH_2)	1464 cm^{-1} [37]
1378	δ_s (CH_3)	1380 cm^{-1} [35]
966	*trans* δ (−CH═)	970 cm^{-1} [36]
794	δ (NH_2)	787 cm^{-1} [37]
722	δ (CH_2)	720 cm^{-1} [35]
661	ν (C−Cl)	830−560 cm^{-1} [35]

661 cm^{-1}.[35] This observation tells us that one of the liquid-phase reactions involves the chlorination of either the methyl (−CH_3), methylene (−CH_2) or methine (=CH) groups in the hydrocarbon chain of the oleylamine molecule. This is consistent with the identification of $[Cl{-}C_{18}H_{36}N{-}H]^+$ observed in the MALDI spectra of the supernatant of the reaction mixture. Also, the absence of the N−H stretching mode (around 3337 cm^{-1}) points to the coordination of the amine group to the surface of the CISe nanocrystals.

Chlorination of hydrocarbons with Cl_2 via radical formation in the presence of UV light or heat has been extensively studied.[38] The formation of chlorinated alkylamines with multiple chlorine atoms on the same hydrocarbon chain cannot be ruled out, but due to the vast excess of oleylamine molecules in comparison to the number of chlorine atoms (approximately 15:1 ratio) in the reaction mixture, a higher yield of monochlorinated amines is expected. Also, it is quite possible that either of precursors (CuCl[39] or $InCl_3$), or any of the reaction intermediates, might be catalyzing the chlorination reaction. The chlorination of the amine group is another pathway by which the reaction might take place, but the higher availability of the hydrocarbon groups (18:1 number ratio of combined methyl, methylene, and methine groups to amine group) may result in a lower rate for that pathway.

The MALDI spectrum of the reaction supernatant at the end of the reaction (chalcopyrite nanocrystals synthesis) also revealed the presence of dioleylamine (secondary amine with the molecular formula $(C_{18}H_{35})_2N{-}H$ corresponding to the m/z ratio of 518.6). This molecule was formed upon the reaction between two oleylamine molecules with the release of NH_3 as the byproduct. The purge gas (argon) exhaust from the reaction was bubbled through distilled water and the pH of the solution was analyzed during the reaction as a function of time to check for the acidic/basic nature of the gaseous byproduct of the reaction. The pH did not change significantly until the temperature of the reaction mixture reached 275 °C, after which the pH increased from 7 to 10 over a period of 15 min. This lends support to the evolution of ammonia due to the dimerization reaction of oleylamine at higher temperatures. However, it is still not very clear if this reaction plays a significant role in the overall formation pathway.

Based on the formation of the chlorinated oleylamine compound and oleylamine hydrochloride salt (upon reaction of HCl with oleylamine) as observed from the MALDI and FTIR experiments, the overall reaction for the formation of $CuInSe_2$ nanocrystals is

$$CuCl + InCl_3 + 2Se + 2R_1{-}CH_2{-}R_2 \rightarrow CuInSe_2 + 2R_1{-}CHCl{-}R_2 + 2HCl \quad (2)$$

where the molecule $R_1{-}CH_2{-}R_2$ is oleylamine. The hydrochloric acid formed in the reaction mixture then readily reacts with the excess oleylamine to form the amine−hydrochloride salt by the following reaction:

$$R_1{-}CH_2NH_2 + HCl \rightarrow R_1{-}CH_2NH_3^+Cl^- \quad (3)$$

where R_1 is $-C_{17}H_{33}$ in the oleylamine molecule.

$CuInSe_2$ nanocrystals have also been synthesized using salts of copper of indium other than the chlorides. The formation pathway with iodide, acetate and acetylacetonate (acac) salts of the metals should be determined by experimentally detecting the intermediates of the reaction. Since the conjugate acids of both the iodide and acetate ions are quite thermodynamically favored products, the formation of hydroiodic acid and acetic acid respectively are very likely possibilities. The oxidation of the $-CH_2{-}NH_2$ group (in oleylamine) to −CH═NH or −C≡N is another possible pathway through which the reaction may take place.[40] The side product with the acac precursors would very likely be the acetylacetonate molecule formed a similar mechanism.[41]

3.2. Reaction in Non-coordinating Solvents. Nanocrystal synthesis experiments were carried out in non-coordinating solvents to verify the role of the solvent as a reactant and to determine the effects of chemisorption of coordinating solvents in the formation pathway. Based on the proposed formation pathway in reaction 2, it was expected that $CuInSe_2$ nanocrystals would be formed in solvents without any metal coordinating groups, since it is the presence of the hydrocarbon groups that is the critical requirement for the reaction to take place. Therefore

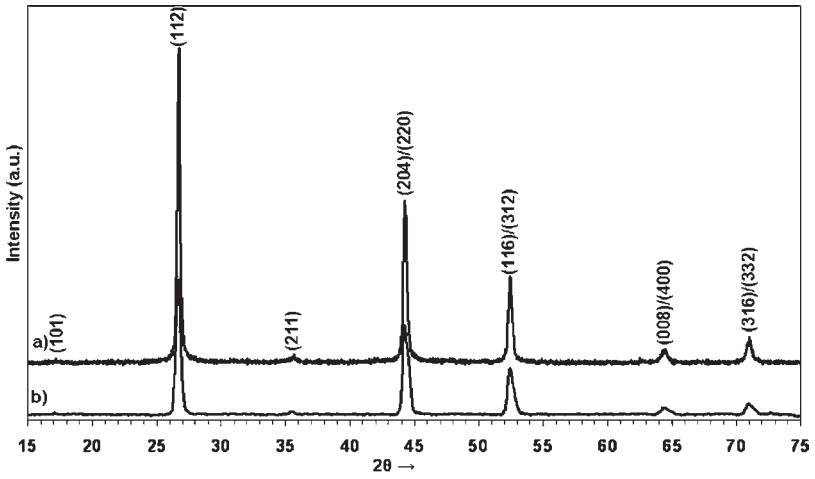

Figure 3. PXRD spectra of $CuInSe_2$ nanocrystals synthesized in (a) 1-octadecene and (b) octadecane using a similar synthesis route as that for oleylamine.

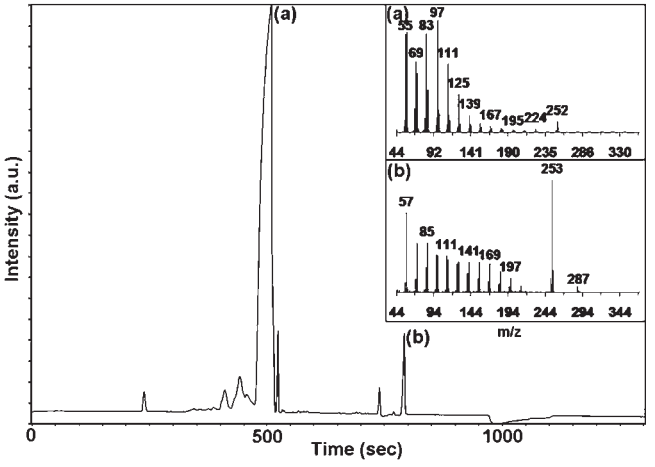

Figure 4. Gas chromatogram and mass spectrum of the reaction supernatant for the synthesis of CISe in 1-octadecene collected at 155 °C. Insets (a) and (b) shows the mass spectra of the peaks (a) and (b) labeled in the GC at retention times of 511 and 792 s, respectively.

the synthesis recipe involving oleylamine was used to test the formation of $CuInSe_2$ nanocrystals in solvents with and without the alkene double bond and the amine group. Indeed our synthesis efforts in 1-octadecene and octadecane resulted in chalcopyrite-structured CISe nanoparticles as observed from the presence of the (211) and (101) secondary peaks (Figure 3). This is in contrast to a previous report in literature that states the necessity of the presence of a coordinating ligand for the formation of $CuInSe_2$ nanoparticles in a non-coordinating solvent like 1-octadecene.[31]

As expected, the CISe nanoparticles synthesized in 1-octadecene and octadecane had irregular morphologies and a wide size distribution and did not disperse well in organic solvents due to the absence of any metal-coordinating functional groups (e.g., amine).

To check the consistency of the formation pathway for the synthesis in 1-octadecene, the reaction supernatant collected at 155 °C was analyzed using gas chromatography−mass spectrometry. The mass spectrum shown in Figure 4a indicates the presence of unreacted 1-octadecene (m/z = 252, and its corresponding fragments at lower m/z ratios) which eluted at a retention time of 511 s. In addition, a chlorinated compound of 1-octadecene corresponding to m/z ratio of 287 and an isotope at 289 (which correspond to the isotopes of the chlorine atom (35 and 37) in the molecule $[C_{18}H_{35}Cl-H]^+$) as shown in Figure 4b was detected in the reaction mixture which eluted at a retention time of 792 s. Similarly, the GC-MS spectrum of the reaction supernatant of the nanocrystal synthesis in octadecane revealed the formation of the chlorinated compound of octadecane as a byproduct of the reaction. This further confirms that the presence of the methyl, methylene, and methine groups is the only necessary requirement for the formation of CISe nanocrystals. However there was no direct evidence of the formation of HCl in the nanocrystal syntheses conducted in 1-octadecene or octadecane. The exhaust purge gas from the reactor was bubbled into a beaker containing water, whose pH was monitored as a function of the time and reaction temperature. The measured pH did not decrease as expected for the amount of HCl generated in the reaction. It is quite possible that all the chlorine atoms from the precursors reacted with the hydrocarbon chain in the solvent, hence forming the chlorinated compound and resulting in evolution of H_2 gas. The molar ratio of chlorinated octadecene to unreacted 1-octadecene (as quantified from the GC of the reaction supernatant in Figure 4b, details in Materials and Methods section) is around 0.03. Assuming that all the chlorine from the precursors gets converted to chlorinated octadecene, that molar ratio should be 0.13. This observation could be possibly explained by the lower yield (40−60%) of nanocrystals in 1-octadecene resulting in lower conversion of the precursors. Also, it is quite possible that some of the chlorinated octadecene interacts with and adsorbs to the surface of the nanocrystals, hence resulting in its lower concentration in the liquid phase of the reaction mixture

3.3. Formation of $CuInSe_2$ Nanocrystals. In the chalcopyrite CISe synthesis in oleylamine, aliquots of the reaction mixture were extracted at various temperatures. The solid precipitates from these aliquots were separated from the supernatants by centrifugation and analyzed using PXRD as shown in Figure 5.

As soon as all the three precursors are added at 130 °C, the formation of (hexagonal phase) γ-CuSe crystals (JCPDS 06-0427) is

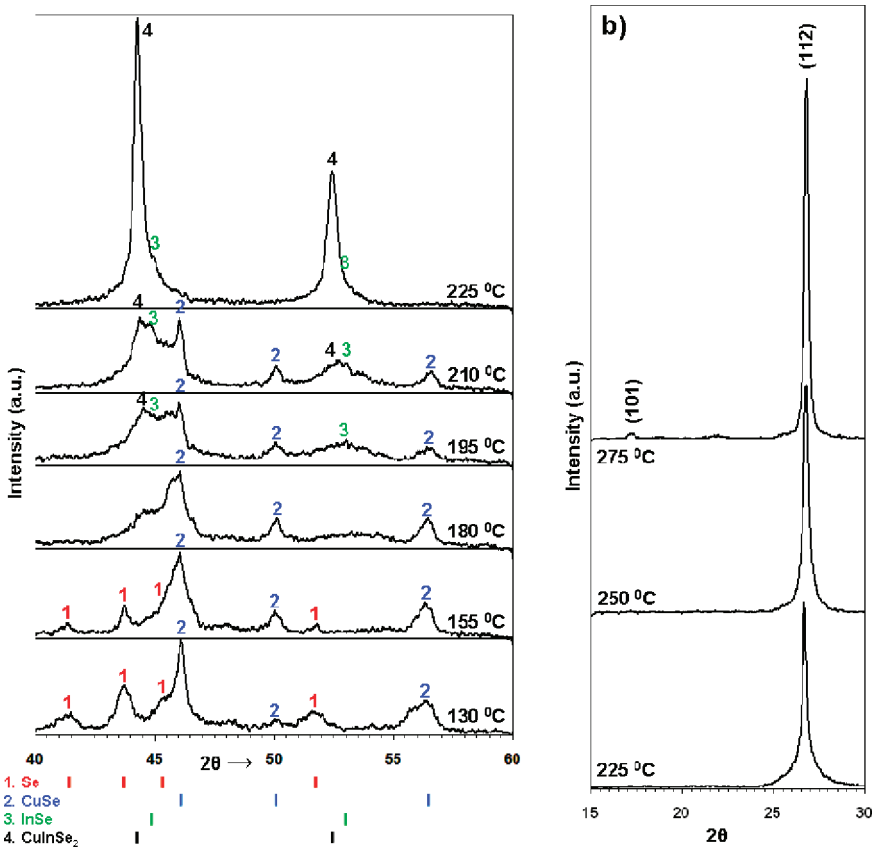

Figure 5. PXRD spectra of the solid intermediates formed during the reaction (a) between 130 and 225 °C and (b) between 225 and 275 °C, showing the (101) and (112) crystallographic planes in chalcopyrite $CuInSe_2$.

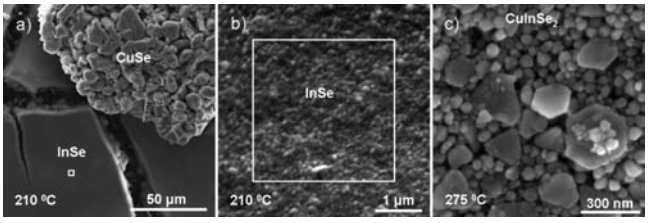

Figure 6. FESEM images of the intermediates formed in the reaction mixture after being extracted at different temperatures. In many cases (210 °C) a bimodal particle size distribution is observed. EDX analysis and size-selective precipitation were used to identify that the larger particle distribution was composed of CuSe while the smaller was composed of InSe. (a) Low-magnification image of solids from extraction at 210 °C. Small InSe nanocrystals are seen beside larger CuSe crystals. (b) Higher magnification image of the region with InSe nanocrystals indicated by the square in part (a). (c) Image showing the chalcopyrite-structured $CuInSe_2$ nanocrystals formed at 275 °C.

observed. At this temperature, unreacted solid selenium (JCPDS 06-0362) is also present in the reaction mixture. As the temperature is increased, the CuSe crystals begin to grow (Figure 6a), and their sizes increase to about 10−30 μm around 210 °C.

At 180 °C, almost none of the selenium remained as a crystalline phase (Figure 5a), as most of it had either reacted with the metal halides or melted in oleylamine[42] (melting point of selenium is 220 °C). Around 195 °C, XRD peaks corresponding to cubic-phase InSe nanocrystals[42] began to appear, and correspondingly nanocrystals of around 50−100 nm diameter could be seen in the SEM images (Figure 6b) of the precipitate collected at 210 °C. Diffraction peaks corresponding to $CuInSe_2$ (JCPDS 40-1487) began to appear around 195 °C as well. Beyond 210 °C, the intensity of CuSe and InSe peaks began to decrease, and correspondingly the sizes of the CuSe and InSe crystals also began to shrink. At 250 °C, $CuInSe_2$ nanocrystals of about 10−15 nm diameter were observed in the FESEM images, and corresponding CISe peaks of higher intensities were also observed in the PXRD. Also, the peak corresponding to the (101) crystallographic plane of the chalcopyrite structure of CISe (JCPDS 40-1487) became more prominent above 250 °C (Figure 5b). The reduction in size of the CuSe and InSe crystals and the appearance of 10−15 nm sized CISe nanocrystals points to the dissolution of formed CuSe and InSe crystals and their reaction in the liquid phase to form CISe nuclei. As the reaction temperature reached 275 °C, the nanocrystals of CISe kept on growing, as seen from SEM images (Figure 6c) and from the sharpening of the peaks in the XRD spectra (Figure 5b). EDX analysis of the precipitate extracted at 210 °C verified the existence of CuSe and InSe nanocrystals which were separated by size-selective precipitation. Based on these observations, i.e., the initial formation of CuSe followed by the formation of InSe and $CuInSe_2$ subsequently around 200 °C, the following step is found to exist in the typical synthesis: CuSe + InSe → $CuInSe_2$.

To verify this step, CuSe and InSe nanocrystals (of the same crystal structure as observed in the intermediates) were synthesized in two separate syntheses (as described in the Materials and Methods section). Then, equimolar ratios of the binary selenides were added to oleylamine at 130 °C, and the reaction mixture was

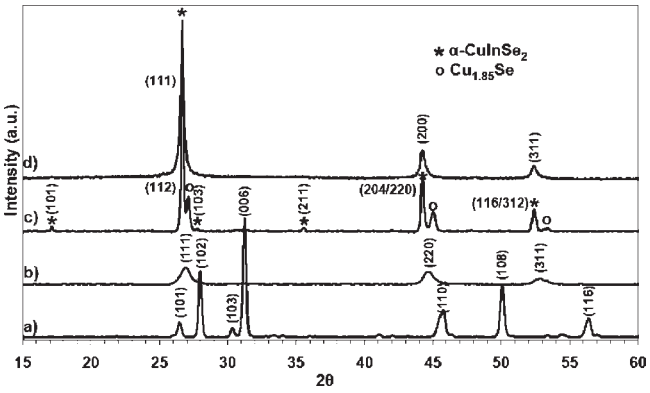

Figure 7. XRD patterns of (a) CuSe crystals, (b) InSe nanocrystals, (c) α-$CuInSe_2$ (chalcopyrite) nanocrystals (and $Cu_{2-x}Se$) as synthesized from the hot injection of $InCl_3$−OLA into a solution containing CuSe nanocrystals, and (d) δ-$CuInSe_2$ (sphalerite) nanocrystals as synthesized from reaction between the CuSe and InSe nanocrystals (from (a) and (b), respectively) in 1:1 molar ratio in oleylamine. Note the presence of the secondary peaks in the chalcopyrite-structured nanocrystals (c) but not in the sphalerite-structured ones (d).

heated to 275 °C and left for 30 min at that temperature, which resulted in δ-$CuInSe_2$ nanocrystals. Figure 7 shows the XRD spectra of the CuSe, InSe, and the resulting δ-$CuInSe_2$ nanocrystals.

The absence of the secondary peaks of the chalcopyrite structure and the calculated ratio of the lattice constants ($c/2a$) of 1.000 ± 0.001 verified the sphalerite crystal structure of the nanocrystals. Binary selenides (CuSe and InSe) deposited by molecular beam expitaxy have also been shown to form $CuInSe_2$.[43] Time-resolved, high-temperature XRD measurements revealed the formation of the sphalerite phase of $CuInSe_2$ without the formation of any other intermediates.[43]

Based on the observations made from the PXRD experiments, the intermediate reactions involved in the formation of $CuInSe_2$ nanocrystals in oleylamine are

$$CuCl(s) + Se(s/l) + 0.5R_1{-}CH_2{-}R_2(l) \rightarrow CuSe(s) + 0.5R_1{-}CHCl{-}R_2(l) + 0.5HCl \quad (4)$$

$$InCl_3(s) + Se(s/l) + 1.5R_1{-}CH_2{-}R_2(l) \rightarrow InSe(s) + 1.5R_1{-}CHCl{-}R_2(l) + 1.5HCl \quad (5)$$

$$CuSe(s) + InSe(s) \rightarrow CuInSe_2(s) \quad (6)$$

where the molecule $R_1{-}CH_2{-}R_2$ is oleylamine.

The aliquot-extraction set of experiments were performed in the chalcopyrite CISe synthesis in 1-octadecene to identify the intermediates formed during the reaction in a purely noncoordinating solvent. Here, $Cu_{2-x}Se$ (JCPDS 06-0680) and In_2Se_3 (JCPDS 40-1407) were observed as the primary reaction intermediates using powder X-ray diffraction techniques. This shows that presence of the coordinating solvent leads to the formation of less energetically favorable indium binary (InSe), whereas the absence of any coordinating solvent results in the formation of the more thermodynamically favorable binary intermediate (In_2Se_3) (standard free energy of formation, $\Delta_f G°_{298}$(InSe) = −112 kJ/mol and $\Delta_f G°_{298}(In_2Se_3)$ = −331 kJ/mol).[44] This again points to the surface-stabilization effect that the coordinating solvent has on the small InSe nanocrystals (Figure 6b), which is absent during the reaction in the noncoordinating solvent.

Table 3. Variation of Reaction Conditions Leading to Different Crystal Structures of $CuInSe_2$[a]

	precursor 3	precursor 4	product
S1	$InCl_3$−OLA	Se in OLA	δ-$CuInSe_2$
T_{add}	130 °C	275 °C	
S2	Se in OLA	$InCl_3$−OLA	α-$CuInSe_2$
T_{add}	130 °C	275 °C	
S3	Se in OLA	$InCl_3$−OLA	δ-$CuInSe_2$
T_{add}	275 °C	275 °C (0 min)	
S4	Se in OLA	$InCl_3$−OLA	α-$CuInSe_2$
T_{add}	275 °C	275 °C (30 min)	

[a] In each synthesis, precursor 1 is oleylamine (OLA) solvent and was added at room temperature. Precursor 2 is CuCl−OLA and was added at 130 °C. The precursors were added in the same order as their number suggests. In syntheses S3 and S4, precursor 4 was added after a specific time (given in brackets) following the addition of precursor 3. T_{add} is the temperature of the reaction mixture at which the precursor is added.

3.4. Effect of the Order of Precursor Addition. Guo et al.[4] report the formation of the disordered sphalerite phase of the CISe nanocrystals upon the hot injection of Se into a solution of CuCl and $InCl_3$ in oleylamine at 285 °C. However, when the Se precursor is added with all the other precursors at 130 °C followed by heating the reactor contents to 285 °C, they report the resulting nanocrystals to have the ordered chalcopyrite structure. We found that the formation of the chalcopyrite crystal structure of $CuInSe_2$ took place primarily due to the solid−liquid reaction between CuSe nanocrystals and the $InCl_3$ dissolved in oleylamine. This was verified by reacting CuSe nanocrystals with $InCl_3$ as the only other reactant (injected at 280 °C and reacted for 30 min) in oleylamine, the resulting product being α-CISe and $Cu_{2-x}Se$ (Figure 6c). It is proposed that some of the CuSe is converted to $Cu_{2-x}Se$, allowing for selenium to go to the formation of $CuInSe_2$ when starting from a 1:1 molar ratio of CuSe and $InCl_3$ (overall selenium deficient). Further experiments were done to prove the hypothesis and are listed in Table 3.

From the results from synthesis S1, it is hypothesized that hot injection of Se−OLA into the halide precursors rapidly leads to the formation of both the binary selenides, which react with each other yielding δ-CISe. However, in synthesis S2, CuCl−OLA and Se in oleylamine react with each other to form CuSe (and a small fraction of $Cu_{2-x}Se$) until the temperature reaches 275 °C, which then reacts with the $InCl_3$−OLA precursor (injected at 275 °C) to form α-CISe. The reaction between $InCl_3$−OLA and the unreacted selenium to yield InSe is feasible, hence the formation of sphalerite $CuInSe_2$ nanocrystals in this synthesis cannot be completely ruled out. In synthesis S3, $InCl_3$−OLA and Se in OLA were injected together into CuCl−OLA at 275 °C leading to δ-CISe, as both the halide precursors react with elemental Se at the same time forming the binary selenides (CuSe and InSe) first. Whereas in synthesis S4, when the injection of $InCl_3$−OLA was delayed by 30 min after the injection of Se in OLA into CuCl−OLA, it allowed the formation of CuSe nanocrystals (in addition to $Cu_{2-x}Se$) which then reacted with $InCl_3$−OLA to form α-CISe nanocrystals.

This explains the effect of the order of the selenium precursor addition on the crystal structure of the resulting CISe nanocrystals.

When Se is injected into a solution of CuCl and $InCl_3$ at 275 °C, the rapid formation of both the binary selenides leaves a very small quantity of unreacted $InCl_3$ to react with CuSe, hence primarily resulting in the sphalerite crystal structure of the nanocrystals. Although the above mechanism is a very likely possibility, the formation of CISe by the direct multibody reaction between the copper, indium and selenium precursors at such high temperatures cannot be ruled out. But, when all the three precursors are added at 130 °C, we observe the formation of CuSe instantly, followed by the formation of InSe beginning around 195 °C (Figure 5a). This allows CuSe to react with unreacted $InCl_3$ at high temperatures resulting in the formation of the ordered and thermodynamically favored chalcopyrite phase of $CuInSe_2$. However, as InSe is also formed at these high temperatures, it would react with some of the existing CuSe hence resulting in the formation of some sphalerite structured nanocrystals. It has also been observed that sphalerite CISe nanocrystal-based films when treated with selenium in oleylamine at 280 °C for longer times (30 min to 1 h) get partially converted to the ordered chalcopyrite crystal structure. This result hints at the relatively slower kinetics of the formation of chalcopyrite CISe from the reaction between CuSe and InSe as compared to the one between CuSe and dissolved In^{3+} in oleylamine. Similar results (slow $CuInSe_2$ formation from CuSe and InSe) are reported in a detailed analysis of the formation pathways of $CuInSe_2$ from solid-state reactions by Hergert et al.,[45] which is explained by the need to break the dication $[In_2]^{4+}$ present in InSe and oxidize the indium to form In^{3+}.

4. CONCLUSIONS

The formation of $CuInSe_2$ nanocrystals from chloride precursors and elemental selenium in oleylamine is preceded by the formation of cuprous selenide (CuSe) and indium selenide (InSe), as detected using X-ray diffraction, electron microscopy, and compositional analysis. It was also found that both the binary selenides were formed from the chloride precursors via the chlorination of the hydrocarbon chain of oleylamine as seen from MALDI mass spectrometry and FTIR spectroscopy. The formation of a very stable molecule such as hydrochloric acid and its acid−base neutralization reaction with oleylamine makes the overall reaction favorable to take place.

Contrary to earlier reports in the literature, and as supported by the proposed nanocrystal formation pathway, $CuInSe_2$ nanocrystals were synthesized in solvents devoid of any metal-coordinating functional groups such as 1-octadecene and octadecane. The chlorination of the hydrocarbon chain of 1-octadecene and octadecane was observed, lending support to the formation pathway observed in oleylamine. However, in the absence of any coordinating solvent, $Cu_{2-x}Se$ and the more thermodynamically favorable binary In_2Se_3 (as compared to InSe) were the intermediates which preceded the formation of $CuInSe_2$. This shows that oleylamine plays a major role in the surface stabilization of the small nanocrystals of InSe, hence making their formation favorable. Also, it was found that the reaction between the binary selenides, CuSe and InSe, primarily resulted in the formation of the disordered sphalerite phase of $CuInSe_2$, however the relatively faster liquid−solid phase reaction between $InCl_3$ and CuSe in the presence of selenium increased the yield of the ordered chalcopyrite crystal structured nanocrystals.

These formation pathway experiments also suggest potential methods to deposit device-quality CISe films (chalcopyrite phase with larger grains), perhaps at lower temperatures. One could perhaps expose a thin film of CuSe nanocrystals to a solution of dissolved $InCl_3$ and Se (a so-called chemical liquid deposition technique). Another potential technique could be to treat a thin film of $CuInSe_2$ or the sulfide ($CuInS_2$) in a solution phase consisting of Se in a dissolved form (a so-called solution selenization technique) to circumvent the high-temperature vapor-phase selenization step.

AUTHOR INFORMATION

Corresponding Author
agrawalr@purdue.edu; h2@uw.edu

ACKNOWLEDGMENT

We thank Debby Sherman for input during the use of the FEI Nova NanoSEM. We also thank Dr. Karl V. Wood and Connie Bonham for the usage of the Applied Biosystems Voyager DE Pro mass spectrometer and the Agilent 5975C gas chromatograph mass spectrometer and helpful discussions for analyzing mass spectrometry results. Discussions with Dr. Qijie Guo are also appreciated.

REFERENCES

(1) Guillemoles, J. F.; Rau, U.; Kronik, L.; Schock, H. W.; Cahen, D. *Adv. Mater.* **1999**, *11*, 957.
(2) Stanbery, B. J. *Crit. Rev. Solid State Mater. Sci.* **2002**, *27*, 73–117.
(3) Repins, I.; Contreras, M. A.; Egaas, B.; DeHart, C.; Scharf, J.; Perkins, C. L.; To, B.; Noufi, R. *Prog. Photovoltaics* **2008**, *16*, 235–239.
(4) Guo, Q.; Kim, S. J.; Kar, M.; Shafarman, W. N.; Birkmire, R. W.; Stach, E. A.; Agrawal, R.; Hillhouse, H. W. *Nano Lett.* **2008**, *8*, 2982–2987.
(5) Guo, Q.; Ford, G. M.; Hillhouse, H. W.; Agrawal, R. *Nano Lett.* **2009**, *9*, 3060–3065.
(6) Guo, Q.; Ford, G. M.; Hillhouse, H. W.; Agrawal, R. Presented at the 34th IEEE Photovoltaics Specialists Conference 2009.
(7) Panthani, M. G.; Akhavan, V.; Goodfellow, B.; Schmidtke, J. P.; Dunn, L.; Dodabalapur, A.; Barbara, P. F.; Korgel, B. A. *J. Am. Chem. Soc.* **2008**, *130*, 16770–16777.
(8) Mitzi, D. B.; Yuan, M.; Liu, W.; Kellock, A. J.; Chey, S. J.; Deline, V.; Schrott, A. G. *Adv. Mater.* **2008**, *20*, 3657.
(9) Hibberd, C. J.; Ernits, K.; Kaelin, M.; Muller, U.; Tiwari, A. N. *Prog. Photovoltaics* **2008**, *16*, 585–593.
(10) Kapur, V. K.; Bansal, A.; Le, P.; Asensio, O. I. *Thin Solid Films* **2003**, *431*, 53–57.
(11) Bhattacharya, R. N.; Batchelor, W.; Granata, J. E.; Hasoon, F.; Wiesner, H.; Ramanathan, K.; Keane, J.; Noufi, R. N. *Sol. Energy Mater. Sol. Cells* **1998**, *55*, 83–94.
(12) Alivisatos, A. P. *J. Phys. Chem.* **1996**, *100*, 13226–13239.
(13) Gur, I.; Fromer, N. A.; Geier, M. L.; Alivisatos, A. P. *Science* **2005**, *310*, 462–465.
(14) Xie, R. G.; Peng, X. G. *Angew. Chem., Int. Ed.* **2008**, *47*, 7677–7680.
(15) Wu, Y.; Wadia, C.; Ma, W. L.; Sadtler, B.; Alivisatos, A. P. *Nano Lett.* **2008**, *8*, 2551–2555.
(16) Mangolini, L.; Thimsen, E.; Kortshagen, U. *Nano Lett.* **2005**, *5*, 655–659.
(17) Peng, Z. A.; Peng, X. G. *J. Am. Chem. Soc.* **2001**, *123*, 183–184.
(18) Murray, C. B.; Norris, D. J.; Bawendi, M. G. *J. Am. Chem. Soc.* **1993**, *115*, 8706–8715.
(19) Carmalt, C. J.; Morrison, D. E.; Parkin, I. P. *J. Mater. Chem.* **1998**, *8*, 2209–2211.

(20) Gurin, V. S. *Colloids Surf. A: Physicochem. Eng Aspects* **1998**, *142*, 35–40.
(21) Schulz, D. L.; Curtis, C. J.; Flitton, R. A.; Wiesner, H.; Keane, J.; Matson, R. J.; Jones, K. M.; Parilla, P. A.; Noufi, R.; Ginley, D. S. *J. Electron. Mater.* **1998**, *27*, 433–437.
(22) Li, B.; Xie, Y.; Huang, J. X.; Qian, Y. T. *Adv. Mater.* **1999**, *11*, 1456–1459.
(23) Malik, M. A.; O'Brien, P.; Revaprasadu, N. *Adv. Mater.* **1999**, *11*, 1441–1444.
(24) Jiang, Y.; Wu, Y.; Mo, X.; Yu, W. C.; Xie, Y.; Qian, Y. T. *Inorg. Chem.* **2000**, *39*, 2964.
(25) Banger, K. K.; Jin, M. H. C.; Harris, J. D.; Fanwick, P. E.; Hepp, A. F. *Inorg. Chem.* **2003**, *42*, 7713–7715.
(26) Castro, S. L.; Bailey, S. G.; Raffaelle, R. P.; Banger, K. K.; Hepp, A. F. *Chem. Mater.* **2003**, *15*, 3142–3147.
(27) Grisaru, H.; Palchik, O.; Gedanken, A.; Palchik, V.; Slifkin, M. A.; Weiss, A. M. *Inorg. Chem.* **2003**, *42*, 7148–7155.
(28) Kaelin, M.; Rudmann, D.; Kurdesau, F.; Meyer, T.; Zogg, H.; Tiwari, A. N. *Thin Solid Films* **2003**, *431*, 58–62.
(29) Chun, Y. G.; Kim, K. H.; Yoon, K. H. *Thin Solid Films* **2005**, *480*, 46–49.
(30) Ahn, S.; Kim, K.; Chun, Y.; Yoon, K. *Thin Solid Films* **2007**, *515*, 4036–4040.
(31) Zhong, H. Z.; Li, Y. C.; Ye, M. F.; Zhu, Z. Z.; Zhou, Y.; Yang, C. H.; Li, Y. F. *Nanotechnology* **2007**, *18*, 025602/1-025602/6.
(32) Tang, J.; Hinds, S.; Kelley, S. O.; Sargent, E. H. *Chem. Mater.* **2008**, *20*, 6906–6910.
(33) Guo, Q.; Agrawal, R.; Hillhouse, H. W. Rapid synthesis of ternary, binary and multinary chalcogenide nanoparticles, WO2008021604A2, 2008.
(34) Roine, A. *Chemical Reaction and Equilibrium Software with Extensive Thermochemical Database*, 5.1 ed.; Outkumpu Research Oy: Pori, Finland, 2002.
(35) Gunzler, H.; Gremlich, H.-U. *IR Spectroscopy*; Wiley-VCH: Weinheim, 2002.
(36) Shukla, N.; Svedberg, E. B.; Ell, J. *Colloids Surf. A: Physicochem. Eng. Aspects* **2007**, *301*, 113–116.
(37) Klokkenburg, M.; Hilhorst, J.; Erne, B. H. *Vibr. Spectrosc.* **2007**, *43*, 243–248.
(38) Taatjes, C. A. *Int. Rev. Phys. Chem.* **1999**, *18*, 419–458.
(39) Bellis, H. E. Melt oxychlorination, US4130595A, 1978.
(40) Chen, M.; Feng, Y.-G.; Wang, X.; Li, T.-C.; Zhang, J.-Y.; Qian, D.-J. *Langmuir* **2007**, *23*, 5296–5304.
(41) Saita, S.; Maenosono, S. *Chem. Mater.* **2005**, *17*, 6624–6634.
(42) Park, K. H.; Jang, K.; Kim, S.; Kim, H. J.; Son, S. U. *J. Am. Chem. Soc.* **2006**, *128*, 14780–14781.
(43) Kim, S.; Kim, W. K.; Kaczynski, R. M.; Acher, R. D.; Yoon, S.; Anderson, T. J.; Crisalle, O. D.; Payzant, E. A.; Li, S. S. *J. Vac. Sci. Technol. A* **2005**, *23*, 310–315.
(44) Cahen, D.; Noufi, R. *J. Phys. Chem. Solids* **1992**, *53*, 991–1005.
(45) Hergert, F.; Jost, S.; Hock, R.; Purwins, M. *J. Solid State Chem.* **2006**, *179*, 2394–2415.